

Article

Thermo-Reversible Gelation of Aqueous Hydrazine for Safe Storage of Hydrazine

Bungo Ochiai *  and Yohei Shimada

Department of Chemistry and Chemical Engineering, Faculty of Engineering, Yamagata University, Jonan 4-3-16, Yonezawa, Yamagata 992-8510, Japan; s.yohey44@gmail.com

* Correspondence: ochiai@yz.yamagata-u.ac.jp; Tel.: +81-238-26-3092

Received: 5 September 2020; Accepted: 9 October 2020; Published: 12 October 2020



Abstract: A reversible gelation–release system was developed for safe storage of toxic hydrazine solution based on gelation at lower critical solution temperature (LCST). Poly(*N*-isopropylacrylamide) (PNIPAM) and its copolymer could form gels of 35wt% hydrazine by dissolution under low temperature and storage at ambient temperatures. For example, PNIPAM gelled a 63 fold heavier amount of 35wt% hydrazine. Aqueous hydrazine was released from the gels by compression or heating, and the gelation–release cycles proceeded quantitatively (> 95%). The high gelation ability and recyclability are suitable for rechargeable systems for safe storage of hydrazine fuels.

Keywords: hydrazine; gel; LCST; fuel cell; poly (*N*-isopropylacrylamide)

1. Introduction

Hydrazine and its derivatives contain high energy and have been applied as fuels and propellants of artificial satellites, space vehicles, and fighter jets [1–5]. Another potential application is a fuel for hydrazine fuel cells (HFCs) [6–19]. HFCs using aqueous solutions with 10%–15% of hydrazine can exhibit outputs as high as those of typical hydrogen fuel cells. Furthermore, the low corrosion of the basic media enables use of accessible materials for both electrocatalysts and electrolyte membranes, namely Co, Ni, Ag, and carbon electrodes and non-fluorine polymer membranes, which cannot be used in hydrogen and methanol fuel cells requiring highly acidic media. The liquid nature makes hydrazine more accessible for consumers by the facile treatment than gaseous fuels. However, the high toxicity and risk of explosion limit the applicability of hydrazine fuels [8,20–22]. Accordingly, methods for safer treatments of hydrazine are highly demanded.

For the safe storage of hydrazine fuels, gelation has been examined to avoid leakage. Some polar polymers such as various polysaccharides serve as gelators for hydrazine and its derivatives [5,23–27]. The gels can be thixotropically transformed to sols fluid enough to be delivered to combustion engines of rockets through pipelines [23–25]. However, the liquids containing the gelators may return to gels again in the pipelines, which can be responsible for clogging up. Due to the loss of the gelators with the fuels, this system is suitable to primary fuel supplying systems, but inapplicable to rechargeable fuel supplying systems. Accordingly, rechargeable systems require reversible immobilization systems employing immobilizing materials remaining in fuel tanks. From this point of view, we developed an efficient gelation system for hydrazine and its aqueous solution based on cross-linked polymers with high affinity to hydrazine [28]. Polyacrylamide, having similarity in structure to hydrazine, was the best polymer for adsorption, and 30–50 fold excess amounts of aqueous hydrazine were immobilized by cross-linked polyacrylamide. The amount of immobilization and the recyclability were superior to chemical immobilization of aqueous hydrazine using cross-linked polymers bearing ketone moieties (2 g of the polymer was used for 0.76 g of 10 wt% aqueous hydrazine) [9]. In addition, the adsorption capacity of the polymer bearing ketone moieties was decreased in the second cycle, probably due to

the irreversible side reaction by the Wolff–Kishner reduction, by which carbonyl groups are reduced to alkanes by hydrazine under basic conditions [29]. Accordingly, adsorption without chemical reactions is desirable for repeated storage. In the course of our study, we found that poly(*N*-isopropylacrylamide) (PNIPAM) is soluble in 35 wt% aqueous hydrazine only under low temperatures. PNIPAM is the most examined polymer with lower critical solution temperature (LCST) behavior, and applied in various fields [30–33]. The transition takes place by the local change of the environment around the isopropyl groups, which are surrounded by water below LCST but in contact with water and the hydrophobic structures in PNIPAM [33]. We accordingly applied this LCST behavior to the reversible gelation of aqueous hydrazine without chemical reactions, and herein report the efficient gelation–release system potentially applicable to the safe storage of aqueous hydrazine for hydrazine fuel cell.

2. Materials and Methods

2.1. Materials

Aqueous solution of hydrazine (35 wt%) and poly(*N*-vinyl pyrrolidone) (PVP) ($M_w = 1,300,000$) were purchased from Aldrich (Missouri, MO, USA), and used without purification. *N*-Isopropylacrylamide (NIPAM) was purchased from Wako Chemical (Tokyo, Japan) and purified by recrystallization with a mixed solvent of hexane and diethyl ether. *N,N*-Dimethylacrylamide (DMAM) was purchased from Wako Chemical, and purified by distillation under reduced pressure in the presence of CaH_2 . Acrylamide (AM) was purchased from Wako Chemical, and purified by recrystallization with methanol. Furthermore, 2,2'-azobisisobutyronitrile (AIBN) was purchased from Tokyo Kasei Kogyo (Tokyo, Japan), and purified by recrystallization with methanol. Anhydrous methanol and 1,4-dioxane used for polymerization were purchased from Kanto Chemical (Tokyo, Japan), and stored under a nitrogen atmosphere. Anhydrous hydrazine (Tokyo Kasei Kogyo) and *N,N*-dimethylformamide (DMF) (Kanto Chemical) were used as received. PNIPAM, poly(*N,N*-dimethyl acrylamide) (PDMAM), and polyacrylamide (PAM) were prepared according to the previously described method [28].

2.2. Instruments

^1H nuclear magnetic resonance (NMR) spectra were recorded on a JEOL (Tokyo, Japan) ECX-400 spectrometer (400 MHz for ^1H) at room temperature. Molecular weight was evaluated by size exclusion chromatography (SEC), measurements were performed on a Tosoh (Tokyo, Japan) HLC-8120 GPC equipped with Tosoh TSK-gel α -M, α -4000, α -3000, and α -2500 tandem columns using *N,N*-dimethylformamide (DMF) containing 10 mM lithium bromide as an eluent at 40 °C. Polystyrene standards (TSK polystyrene standards, Tosoh) were used for calibration. UV-vis (ultraviolet-visible) spectroscopy measurements were performed on a JASCO (Tokyo, Japan) V-630 spectrometer. Fourier transform infrared spectroscopy was measured on a Shimadzu (Kyoto, Japan) IRSpirit spectrometer equipped with a Shimadzu QATR-S attenuated total reflection apparatus.

2.3. Radical Copolymerization of NIPAM with Comonomers (General Procedure)

NIPAM, a comonomer (total monomer amount = 2.50 mmol), and AIBN (5 mg, 1 mol% to total monomers) were added to a polymerization tube containing a magnetic stir bar. Then, 1,4-dioxane (2.5 mL) or methanol (2.5 mL) was added after the tube was filled with nitrogen after evacuation. The tube was degassed and sealed, and the polymerization was conducted at 60 °C for 4 h. The reaction mixture was poured into an excess amount of diethyl ether. The copolymers, poly(NIPAM-*co*-AM) (P(NIPAM-*co*-AM)) and poly(NIPAM-*co*-DMAM) (P(NIPAM-*co*-DMAM)), were obtained by filtration and drying under reduced pressure. The ^1H NMR spectra of the polymers are indicated in Supplementary Materials.

Entry 1: NIPAM = 142 mg (1.25 mmol), AM = 89 mg (1.25 mmol), yield = 201 mg (87%).

Entry 2: NIPAM = 189 mg (1.67 mmol), AM = 59 mg (0.83 mmol), yield = 204 mg (82%).

Entry 3: NIPAM = 257 mg (2.27 mmol), AM = 16 mg (0.23 mmol), yield = 209 mg (77%).

Entry 4: NIPAM = 141 mg (1.25 mmol), DMAM = 84 mg (0.85 mmol), yield = 190 mg (85%).

Entry 5: NIPAM = 235 mg (2.08 mmol), DMAM = 40 mg (0.42 mmol), yield = 250 mg (91%).

Entry 6: NIPAM = 257 mg (2.27 mmol), DMAM = 23 mg (0.23 mmol), yield = 263 mg (94%).

2.4. Gelation of Hydrazine Solution by LCST Gelators (General Procedure)

PNIPAM (40 μ g, 350 μ mol-unit) and 35wt% aqueous hydrazine (2.53 g) were added in a glass vial, and the vial was stored at -20 °C for 24 h. Then, the homogeneous solution was gelled by storing at room temperature.

2.5. Release of Hydrazine from Hydrazine Gel by Compression (Typical Procedure)

PNIPAM (80 μ g, 710 μ mol-unit) and 35wt% aqueous hydrazine (5.05 g) were added to a glass vial, and the vial was stored at -20 °C for 24 h. Then, the homogeneous solution was transferred into a syringe with a cotton filter, and the mixture was gelled at room temperature (amount of hydrazine gel = 2.793 g). Aqueous hydrazine was squeezed off by compression (2.192 g, 79.7%). The concentration of hydrazine (35 wt%) in the squeezed solution was quantified by UV-vis spectroscopy indicated by *p*-dimethylaminobenzaldehyde.

2.6. Release of Hydrazine from Hydrazine Gel by Heating (Typical Procedure)

P(NIPAM-*co*-AM) (40 μ g, 310 μ mol-PNIPAM unit and 70 μ mol-AM unit) and 35wt% aqueous hydrazine (2.50 g) were added in a glass vial, and the vial was stored at -20 °C for 24 h. Then, the homogeneous solution was gelled at room temperature. Aqueous hydrazine was separated out by heating in a thermostat oil bath set at 90 °C. The solution was weighed after removal of the aggregated polymer (2.376 g, 94.9%). The concentration of hydrazine (37 wt%) in the separated solution was quantified by UV-vis spectroscopy indicated by *p*-dimethylaminobenzaldehyde according to the method developed by Gamble and Hoffman [34]. To a vial containing P(NIPAM-*co*-AM) absorbing a trace amount of aqueous hydrazine, 35wt% aqueous hydrazine (2.376 g) with the amount identical to the released solution was added again, and the vial was stored at -20 °C. Repeated experiments were carried out as the first experiment.

3. Results and Discussion

3.1. Phase-Transition Behavior of Aqueous Hydrazine Solution Containing Hydrophilic Polymers

The temperature-dependent phase transfer behavior was investigated for 35 wt% hydrazine aqueous solutions of hydrophilic polymers under a 16 mg/mL concentration of the polymers. The measurements were started from -10 °C, heated to 90 °C at a heating rate of 2 °C/min, and then cooled to -10 °C at a cooling rate of 2 °C/min. The examined polymers are poly(*N*-isopropyl acrylamide) (PNIPAM), poly(*N,N*-dimethyl acrylamide) (PDMAM), poly(vinyl pyrrolidone) (PVP), and polyacrylamide (PAM), which are found soluble in 35 wt% hydrazine in our previous work (Figure 1) [28]. Protic polymers with higher Hildebrand solubility parameters [35] have high affinity with hydrazine, while aprotic hydrophilic polymers and protic polymers with lower solubility parameters have moderate affinity. PNIPAM, the most popular LCST polymer, was initially soluble, but started clouding at -6 °C. The desolvation proceeded rapidly, and the transmittance became zero at -3 °C by gelation (Table 1, Figures 2 and 3). The gel state was retained during the cooling process until -10 °C, indicating the slow solvation of PNIPAM by hydrazine solution. The stability of the gel implies the suitability as the reversible gelation system. The LCST lower than that in aqueous solution and the slow solvation indicate that the affinity of PNIPAM with hydrazine is lower than that with water. By contrast, PDMAM and PVP showed LCST at 53 and 59 °C, respectively, and the solutions were transformed to turbid fluids (discussed later). The turbid fluids after the heating processes turned transparent by the cooling process. The transitions during both heating and cooling were very sharp. The LCST higher than room temperature is not suitable to the reversible gelation system.

The solution of PAM having the solubility parameter closest to 35 wt% hydrazine aqueous solution stayed homogeneous in the examined range. The similarity of the structures led to the high affinity.

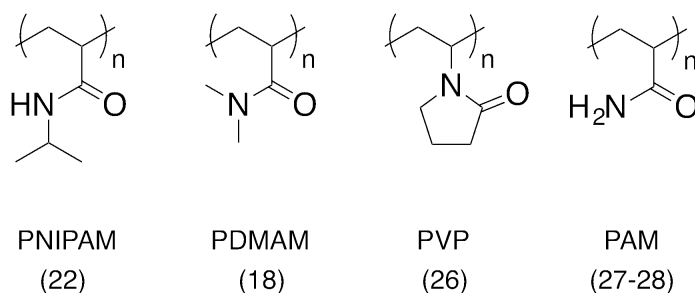


Figure 1. Polymers examined in the phase transition of 35 wt% hydrazine aqueous solutions. The numbers in the parentheses indicate the Hildebrand solubility parameters reported in [35].

Table 1. Phase transition temperatures of 35 wt% hydrazine aqueous solutions of polymers.

Polymer ^a	PNIPAM	PDMAM	PVP	PAM
Heating (°C) ^b	−5	53	59	None
Cooling (°C) ^b	<−10	49	53	None

^a Polymers = 40 mg, 35 wt% hydrazine aqueous solution = 2.53 g. ^b Heating and cooling rate = 2 °C/min, temperatures with 50% absorbance at 650 nm.

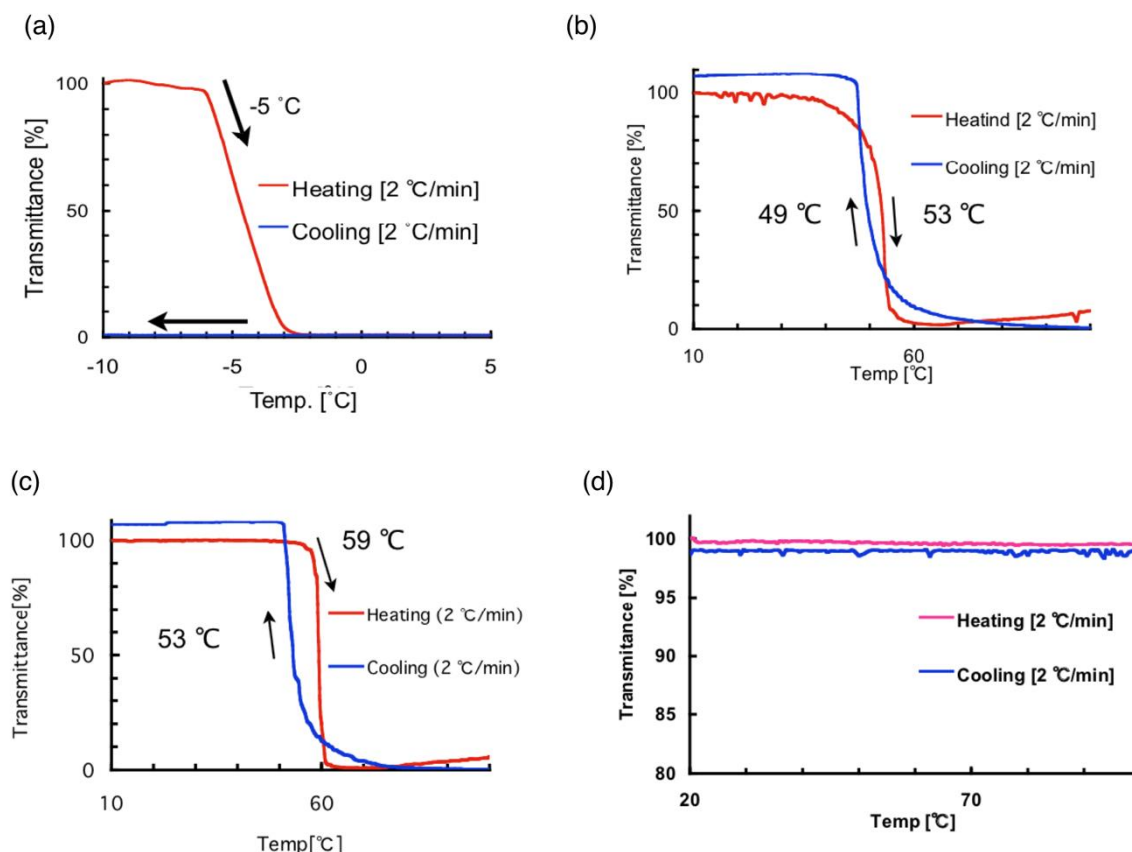


Figure 2. Effect of temperature on transmittance of 35 wt% hydrazine aqueous solutions containing 16 mg/mL of (a) PNIPAM, (b) PDMAM, (c) PVP, and (d) PAM (scan rate = 2 °C/min, pathlength = 10 mm).

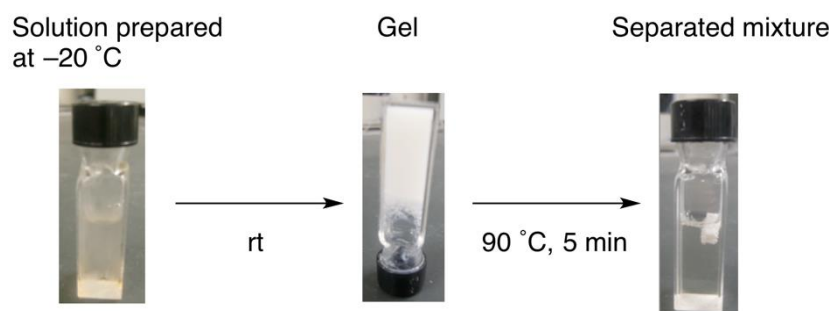
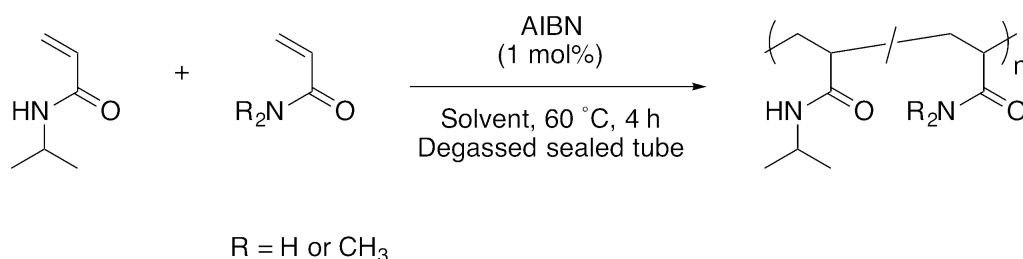


Figure 3. Photo-images of solution prepared at $-20\text{ }^{\circ}\text{C}$, gel prepared at room temperature, and separated mixture prepared by heating at $90\text{ }^{\circ}\text{C}$ of 35 wt% aqueous hydrazine containing 1.6 wt% of PNIPAM. A glass cuvette with dimensions of $45 \times 12.5 \times 12.5\text{ mm}$ was used.

In order to adjust the LCST precisely, copolymers, P(NIPAM-*co*-AM) and P(NIPAM-*co*-DMAM), with various compositions were also prepared (Scheme 1, Table 2). The gelation behaviors were investigated for PNIPAM, P(NIPAM-*co*-AM) and P(NIPAM-*co*-DMAM). Mixtures of 40 mg of polymers and 2.53 g of 35wt% hydrazine aqueous solution were stored at $-20\text{ }^{\circ}\text{C}$ for 24 h to dissolve the polymers. Then, the homogeneous solutions were stored at room temperature. All the solutions became heterogeneous. While PNIPAM and the copolymers with higher compositions of PNIPAM became gel, the copolymers with lower compositions of PNIPAM became turbid fluids (Figure 3, Table 3). The effect of AM was stronger than the effect of DMAM due to the higher affinity of AM and hydrazine, clearly indicated by the absence of LCST of hydrazine solution of AM. The hydrazine affinity of the DMAM unit, stronger than that of the PNIPAM unit but weaker than that of the AM unit, resulted in a weaker effect on the transition temperature.



Scheme 1. Radical copolymerization of NIPAM and comonomers.

Table 2. Synthesis of P(NIPAM-*co*-AM) and P(NIPAM-*co*-DMAM) by radical polymerization of NIPAM and comonomers.

Entry	Comonomer	Solvent	[NIPAM] ₀ /[Comonomer] ₀	Copolymer Composition (NIPAM/Comonomer) ^a	Yield (%) ^b	M _n (M _w /M _n) ^c
1	AM	MeOH	50/50	49/51	87	6300 (1.4)
2	AM	MeOH	67/33	56/44	82	62,700 (2.6)
3	AM	MeOH	91/9	80/20	77	62,200 (3.2)
4	DMAM	DOX	60/40	39/61	85	37,400 (3.2)
5	DMAM	DOX	83/17	60/40	91	46,100 (2.7)
6	DMAM	DOX	91/9	75/25	93	47,800 (3.6)

Conditions: $60\text{ }^{\circ}\text{C}$, total molar amounts of monomers = 2.50 mmol, solvent = 2.5 mL, 2,2'-azobisisobutyronitrile (AIBN) = 30 μmol , degassed sealed tube. ^a Determined by ^1H NMR spectroscopy (D_2O , 400 MHz). ^b Isolated yield after precipitation with diethyl ether. ^c Estimated by size exclusion chromatography (SEC) (polystyrene standards, *N,N*-dimethylformamide (DMF) containing 10 mM LiBr).

Table 3. Gelation and phase transition behaviors of P(NIPAM-co-AM) and P(NIPAM-co-DMAM) in 35wt% hydrazine aqueous solution.

Copolymer	Copolymer Composition (NIPAM/Co monomer) ^a	State at Temperature Higher than Transition Temperature	Transition Temperature (°C) ^b	
			Heating	Cooling
P(NIPAM-co-AM)	36/61	Turbid fluid	−1	−7
	60/40	Gel	−1	−9
	75/25	Gel	<−10	<−10
P(NIPAM-co-DMAM)	49/51	Turbid fluid	69	60
	56/44	Turbid fluid	32	28
	80/20	Gel	4	−9

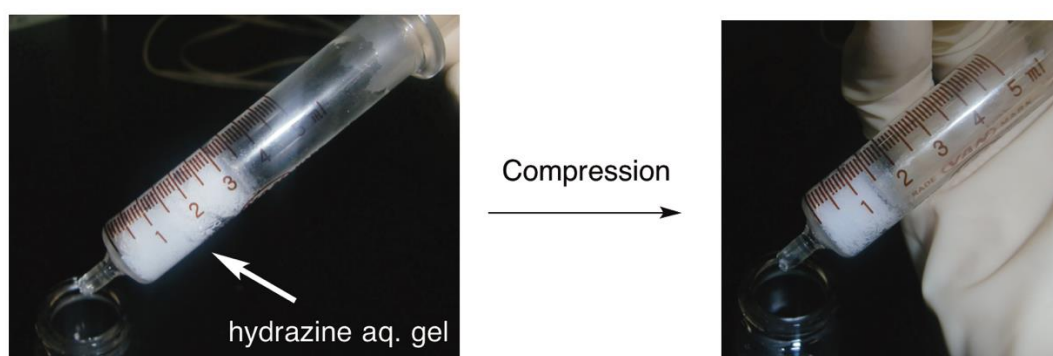
Conditions: the mixture of polymer (40 mg) and 35 wt% hydrazine aqueous solution was stored at −20 °C for 24 h, and the resulting solution was warmed to room temperature. ^a Determined by ¹H NMR spectroscopy (D₂O, 400 MHz). ^b Measured by UV-vis spectroscopy (transmittance at 650 nm, scanning rate = 2 °C/min).

A probable reason for the unsuccessful gelation by the polymers resulting in turbid fluids is the higher transition temperature. The gelation at LCST requires moderate interactions between the gelator and the media, which can be attained by moderate molecular motion preventing solvation and allowing weak interactions. At high temperatures, the molecular motion becomes vigorous and the interactions between the media and the polymers are prohibited. As a result, the polymers are phase-separated from the aqueous solution of hydrazine.

3.2. Release of Aqueous Hydrazine Solution from LCST Gels

3.2.1. Release of Aqueous Hydrazine Solution by Compression

The gel of 35 wt% hydrazine aqueous solution gelled by 1.6 wt% of PNIPAM was subjected to the release of hydrazine solution by mechanical compression (Figure 4). The gel was prepared in a glass syringe containing the cold hydrazine solution containing PNIPAM by storing at room temperature. The gel was compressed by manually pushing the plunger, in an identical manner to the previous work. The compression released 79.7% of hydrazine solution, and the rest of the hydrazine solution was retained in the gel. The concentration of hydrazine in the released solution was 35 wt%, namely the same concentration as the original solution, as quantified by UV-vis measurements indicated by *p*-dimethylaminobenzaldehyde, although there were differing strengths in the interactions of PNIPAM with water and hydrazine. The identical concentration originates from the very trace amount of PNIPAM in the gel that does not affect the concentration of hydrazine.

**Figure 4.** Releasing of hydrazine from hydrazine gel by compression.

3.2.2. Release of Aqueous Hydrazine Solution by Heating

Hydrazine was released by heating the gels. Stable gels from PNIPAM and P(PIPAM-co-AM) (80/20) were evaluated, and 1.6 wt% of the gelators was used (Table 4). The gels were heated for 5 min at 90 or 60 °C, and the gel was transformed into solid and liquid (Figure 3). The heating at 90 °C resulted

in high release efficiencies for both, and the concentrations of hydrazine in the released solution were almost identical to the initial concentration. The heating at 60 °C resulted in lower release efficiencies by the partial phase separation and slightly higher concentrations of hydrazine. This predominant release of hydrazine agrees well with the LCSTs of aqueous hydrazine lower than those of aqueous solutions. The release at 60 °C suggests the limitation of this system for use at high temperatures.

Table 4. Release of hydrazine by heating of gels of 35wt% hydrazine aqueous solution.

Polymer	Temp. (°C)	Hydrazine Release Ratio (%) ^a	Hydrazine Concentration (wt%) ^b
PNIPAM	90	93	35
	60	47	43
P(NIPAM-co-AM) (NIPAM/AM = 80/20)	90	95	37
	60	68	38

Conditions: the mixture of polymer (40 mg) and 35wt% hydrazine aqueous solution was stored at −20 °C for 24 h, and the resulting solution was warmed to room temperature. Then, the gel was heated for 5 min. ^a Determined by weight loss of gel. ^b Measured by UV-vis spectroscopy indicated by *p*-dimethylaminobenzaldehyde.

The recyclability was examined for P(NIPAM-co-AM), exhibiting better releasing ability (Table 5). Hydrazine gel was heated at 90 °C for 5 min to release hydrazine, and the residual solid was subjected to the gelation again by adding aqueous hydrazine followed by cooling to −20 °C. This cycle was conducted three times. The excellent gelation and releasing abilities were retained for three times, indicating the high recyclability suitable to rechargeable systems. The slight increase in the hydrazine concentration implies that the higher affinity of AM with water resulted in the residual water in the remained gel.

Table 5. Recycling of P(NIPAM-co-AM) gelator for 35wt% hydrazine in releasing by heating at 90 °C for 5 min.

Cycle	Polymer/Hydrazine aq. (w/w) ^a	Hydrazine Release Ratio (%) ^b	Hydrazine Concentration (wt%) ^c
1	1/63	95	37
2	1/63	96	36
3	1/63	95	39

Conditions: the mixture of polymer (40 mg) and 35 wt% hydrazine aqueous solution was stored at −20 °C for 24 h, and the resulting solution was warmed to room temperature. Then, the gel was heated at 90 °C for 5 min. ^a Measured by weight of hydrazine gel. ^b Determined by weight loss of gel. ^c Measured by UV-vis spectroscopy indicated by *p*-dimethylaminobenzaldehyde.

We investigated the effect of hydrazine on the LCST gelation induced by polyacrylamide derivatives by FTIR spectroscopy. The FTIR spectra of the solutions and the gels were almost identical and the signals originating from the polymers were unobservable due to the low concentration. We accordingly investigated the interaction of amide moieties with water and hydrazine employing DMF as a model amide (Figure 5). The absorption of the stretching vibration of the carbonyl group of pristine DMF was observed at 1651 cm^{−1}. The carbonyl absorption of DMF mixed with water (v/v = 1/1) shifted to 1647 cm^{−1} by the hydrogen bonding with the proton of water reducing the sp² character of the carbonyl group. By contrast, the carbonyl absorption of DMF mixed with hydrazine (v/v = 1/1) was observed at 1660 cm^{−1}, indicating that the N–H group in hydrazine did not interact with the carbonyl group in DMF. The absorption of the N–H stretching vibration also supported the negligible interaction between hydrazine and DMF (Figure 5b). The N–H absorption peaks of hydrazine were observed at 3333 and 3189 cm^{−1}, indicating the strong hydrogen bonding, and these wavenumbers are identical to those of hydrazine mixed with DMF observed at 3340 and 3193 cm^{−1}. The N–H absorption of aqueous hydrazine was observed at 3453 cm^{−1} in the range of weakly hydrogen-bonded N–H moieties, originating from the hydrogen bonding between the strongly basic nitrogen in hydrogen and O–H protons of water having higher acidity than N–H protons of hydrazine.

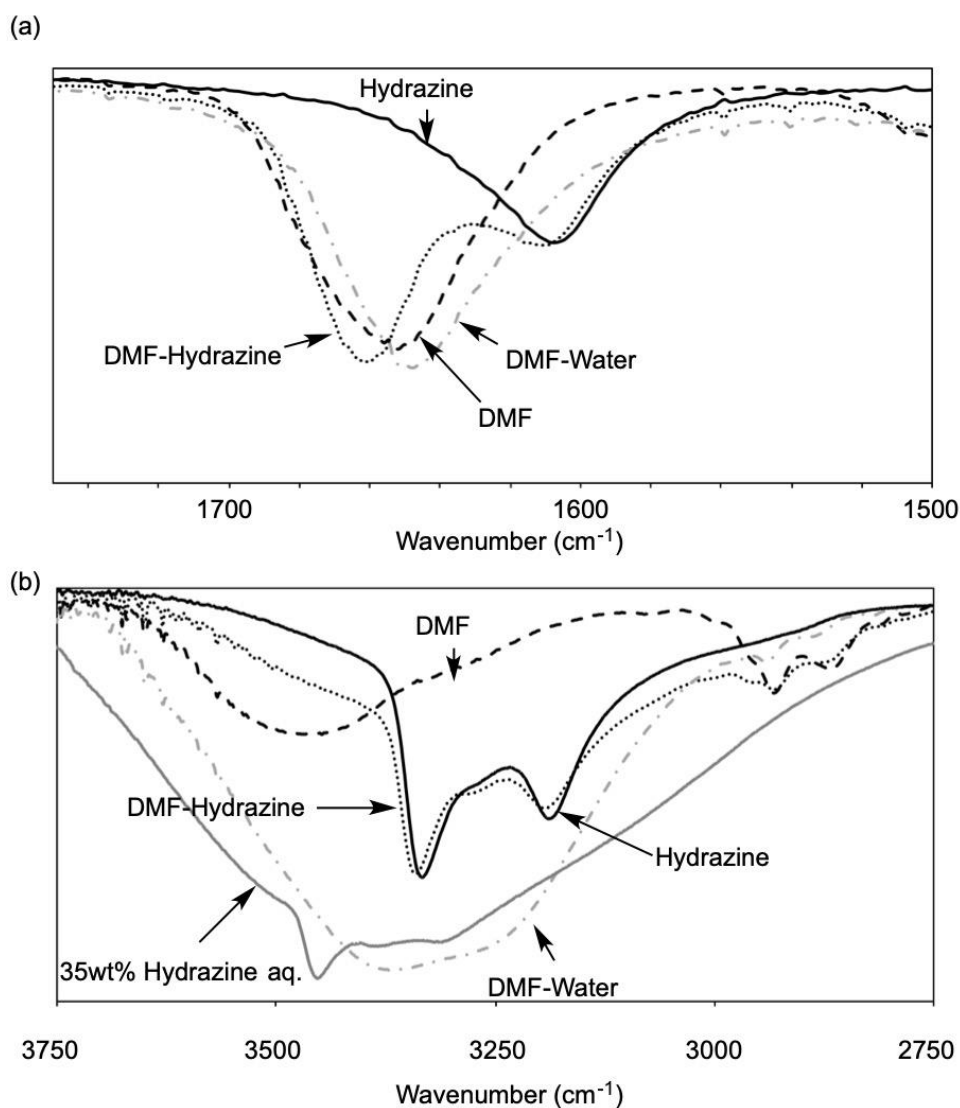


Figure 5. FTIR spectra of DMF, a mixture of DMF and hydrazine ($v/v = 1/1$), a mixture of DMF and water ($v/v = 1/1$), and hydrazine for (a) carbonyl and (b) N–H regions.

These results indicate that the interaction of Lewis-basic hydrazine with Lewis-basic amide moieties is weaker than the interaction of water with amide moieties. The weaker interaction means the lower affinity of hydrazine with amide moieties, which leads to the weaker solvation of amide moieties by hydrazine. This weaker solvation of amide moieties by hydrazine is ascribable to the affinity of the examined polyacrylamide derivatives with aqueous hydrazine being lower than that with water, resulting in the LCST of the solutions of the polyacrylamide derivatives in aqueous hydrazine lower than the LCST in water.

4. Conclusions

We developed a reversible gelation system for aqueous hydrazine based on LCST gelation induced by polyacrylamide derivatives occurring at lower temperatures than LCST in water. The affinity between amide moieties with hydrazine being weaker than that with water is the plausible result of the LCST in aqueous hydrazine being lower than the LCST in water. Gels of 35 wt% aqueous hydrazine were formed by warming solutions of PNIPAM and its copolymers in aqueous hydrazine prepared under cold conditions. Less than 2 wt% of the polymers were enough for sufficient gelation. Aqueous

hydrazine could be released by compression at ambient temperature and heating. The recyclability and high gelation ability are suitable to provide safe rechargeable fuel systems for hydrazine fuels.

Supplementary Materials: The following are available online at <http://www.mdpi.com/2227-7080/8/4/53/s1>, Figure S1: ^1H NMR spectra of polymers (400 MHz, D_2O , rt).

Author Contributions: Conceptualization, B.O.; methodology, B.O. and Y.S.; validation, B.O. and Y.S.; formal analysis, Y.S.; investigation, Y.S.; resources, Y.S.; data curation, Y.S.; writing, B.O.; visualization, B.O.; supervision, B.O.; project administration, B.O.; funding acquisition, B.O. All authors have read and agreed to the published version of the manuscript.

Funding: This research received no external funding.

Conflicts of Interest: The authors declare no conflict of interest.

References

1. McNutt, R.L., Jr.; Solomon, S.C.; Gold, R.E.; Leary, J.C. The MESSENGER Team, The MESSENGER mission to Mercury: Development history and early mission status. *Adv. Space Res.* **2006**, *38*, 564–571. [[CrossRef](#)]
2. Leary, J.C.; Conde, R.F.; Dakermanji, G.; Engelbrecht, C.S.; Ercol, C.J.; Fielhauer, K.B.; Grant, D.G.; Hartka, T.J.; Hill, T.A.; Jaskulek, S.E.; et al. The MESSENGER spacecraft. *Space Sci. Rev.* **2007**, *131*, 187–217. [[CrossRef](#)]
3. Jain, S.R. Self-igniting Fuel-oxidizer Systems and Hybrid Rockets. *J. Sci. Ind. Res.* **2003**, *62*, 293–310.
4. Lai, K.Y.; Zhu, R.S.; Lin, M.C. Why mixtures of hydrazine and dinitrogen tetroxide are hypergolic? *Chem. Phys. Lett.* **2012**, *537*, 33–37. [[CrossRef](#)]
5. Solomon, Y.; DeFini, S.J.; Pourpoint, T.L.; Anderson, W.E. Gelled Monomethyl Hydrazine Hypergolic Droplet Investigation. *J. Propul. Power* **2013**, *29*, 79–86. [[CrossRef](#)]
6. Evans, G.E.; Kordes, K.V. Hydrazine-air fuel cells. *Hydrazine-air fuel cells emerge from the laboratory. Science* **1967**, *158*, 1148–1152. [[CrossRef](#)]
7. Meibuhr, S.G. Surface-Catalyzed Anodes for Hydrazine Fuel Cells I. Preparation of the Substrate. *J. Electrochem. Soc.* **1974**, *121*, 1264–1270. [[CrossRef](#)]
8. Demirci, U.B. Direct liquid-feed fuel cells: Thermodynamic and environmental concerns. *J. Power Sources* **2007**, *169*, 239–246. [[CrossRef](#)]
9. Asazawa, K.; Yamada, K.; Tanaka, H.; Oka, A.; Taniguchi, M.; Kobayashi, T. A platinum-free zero-carbon-emission easy fueling direct hydrazine fuel cell for vehicles. *Angew. Chem. Int. Ed.* **2007**, *46*, 8024–8027. [[CrossRef](#)]
10. Asazawa, K.; Sakamoto, T.; Yamaguchi, S.; Yamada, K.; Fujikawa, H.; Tanaka, H.; Oguro, K. Study of anode catalysts and fuel concentration on direct hydrazine alkaline anion-exchange membrane fuel cells. *J. Electrochem. Soc.* **2009**, *156*, B509–B512. [[CrossRef](#)]
11. Serov, A.; Kwak, C. Direct hydrazine fuel cells: A review. *Appl. Cat. B Environ.* **2010**, *98*, 1–9. [[CrossRef](#)]
12. Rees, N.; Compton, R. Carbon-free energy: A review of ammonia- and hydrazine-based electrochemical fuel cells. *Energy Environ. Sci.* **2011**, *4*, 1255–1260. [[CrossRef](#)]
13. Tanaka, M.; Fukasawa, K.; Nishino, E.; Yamaguchi, S.; Yamada, K.; Tanaka, H.; Bae, B.; Miyatake, K.; Watanabe, M. Anion conductive block poly(arylene ether)s: Synthesis, properties, and application in alkaline fuel cells. *J. Am. Chem. Soc.* **2011**, *133*, 10646–10654. [[CrossRef](#)] [[PubMed](#)]
14. Sanabria-Chinchilla, J.; Asazawa, K.; Sakamoto, T.; Yamada, K.; Tanaka, H.; Strasser, P. Noble metal-free hydrazine fuel cell catalysts: EPOC effect in competing chemical and electrochemical reaction pathways. *J. Am. Chem. Soc.* **2011**, *133*, 5425–5431. [[CrossRef](#)] [[PubMed](#)]
15. Granot, E.; Filanovsky, B.; Presman, I.; Kuras, I.; Patolsky, F. Hydrazine/air direct-liquid fuel cell based on nanostructured copper anodes. *J. Power Sources* **2012**, *204*, 116–121. [[CrossRef](#)]
16. Lan, R.; Irvine, J.T.S.; Tao, S. Ammonia and related chemicals as potential indirect hydrogen storage materials. *Int. J. Hydrog. Energy* **2012**, *37*, 1482–1494. [[CrossRef](#)]
17. Yan, X.; Meng, F.; Xie, Y.; Liu, J.; Ding, Y. Direct $\text{N}_2\text{H}_4/\text{H}_2\text{O}_2$ fuel cells powered by nanoporous gold leaves. *Sci. Rep.* **2012**, *2*, 941. [[CrossRef](#)] [[PubMed](#)]
18. Yang, H.; Zhong, X.; Dong, Z.; Wang, J.; Jin, J.; Ma, J. A highly active hydrazine fuel cell catalyst consisting of a Ni-Fe nanoparticle alloy plated on carbon materials by pulse reversal. *RSC Adv.* **2012**, *2*, 5038–5040. [[CrossRef](#)]

19. Akbar, K.; Kim, J.; Lee, Z.; Kim, M.; Yi, Y.; Chun, S. Superaerophobic graphene nano-hills for direct hydrazine fuel cells. *NPG Asia Mater.* **2017**, *9*, e378. [[CrossRef](#)]
20. Choudhary, G.; Hansen, H. Human health perspective on environmental exposure to hydrazines: A review. *Chemosphere* **1998**, *37*, 801–843. [[CrossRef](#)]
21. Ritz, B.; Zhao, Y.; Krishnadasan, A.; Kennedy, N.; Morgenstern, H. Estimated effects of hydrazine exposure on cancer incidence and mortality in aerospace workers. *Epidemiology* **2006**, *17*, 154–161. [[CrossRef](#)] [[PubMed](#)]
22. Kao, Y.H.; Chong, C.H.; Ng, W.T.; Lim, D. Hydrazine inhalation hepatotoxicity. *Occup. Med.* **2007**, *57*, 535–537. [[CrossRef](#)] [[PubMed](#)]
23. Fujiyoshi, H.; Kubota, N.; Ayabe, T. A feeding method and a supply device of gelling propellant. JP. Patent No. P4,075,133, 8 February 2008. (In Japanese). Available online: <https://www.j-platpat.inpit.go.jp/c1800/PU/JP-4075133/776924ED588A88F70442DB28E6D592C52B7C86A37328570C3C0D33F412B97BAE/15/ja> (accessed on 30 July 2020).
24. Rahimi, S.; Hasan, D.; Perets, A. Development of laboratory-scale gel-propulsion technology. *J. Propuls. Power* **2004**, *20*, 93–100. [[CrossRef](#)]
25. Rahimi, S.; Perets, A.; Natan, B. Rheological Matching of Gel Propellants. *J. Propul. Power* **2010**, *26*, 376–379. [[CrossRef](#)]
26. Dennis, J.D.; Kubal, T.D.; Campanella, O.; Son, S.F.; Pourpoint, T.L. Rheological characterization of monomethylhydrazine gels. *J. Propul. Power* **2013**, *29*, 313–320. [[CrossRef](#)]
27. Dennis, J.D.; Willits, J.D.; Pourpoint, T.L. Performance of neat and gelled monomethylhydrazine and red fuming nitric acid in an unlike-doublet combustor. *Combust. Sci. Technol.* **2018**, *190*, 1141–1157. [[CrossRef](#)]
28. Ochiai, B.; Shimada, Y. Reversible gelation system for hydrazine based on polymer absorbent. *Technologies* **2018**, *6*, 80. [[CrossRef](#)]
29. Lewis, D. *The Wolff-Kishner Reduction and Related Reactions*; Elsevier: Amsterdam, The Netherlands, 2019; ISBN 9780128157275.
30. Schild, H.G. Poly(*N*-isopropylacrylamide) -experiment, theory, and application. *Prog. Polym. Sci.* **1992**, *17*, 163–249. [[CrossRef](#)]
31. Gil, E.S.; Hudson, S.M. Stimuli-responsive polymers and their bioconjugates. *Prog. Polym. Sci.* **2004**, *29*, 1173–1222. [[CrossRef](#)]
32. Qiao, S.; Wang, H. Temperature-responsive polymers: Synthesis, properties, and biomedical applications. *NANO Res.* **2018**, *11*, 5400–5423. [[CrossRef](#)]
33. Pelton, R. Poly(*N*-isopropylacrylamide) (PNIPAM) is never hydrophobic. *J. Colloid Interface Sci.* **2010**, *348*, 673–674. [[CrossRef](#)] [[PubMed](#)]
34. Gamble, D.S.; Hoffman, I. Photometric analysis of trace amounts of hydrazine with *p*-dimethylaminobenzaldehyde. Chemical equilibria. *Canadian J. Chem.* **1967**, *45*, 2813–2819. [[CrossRef](#)]
35. Barton, A.F.M. *Handbook of Polymer-Liquid Interaction Parameters and Solubility Parameters*; CRC Press: Boca Raton, FL, USA, 1990; ISBN 0-8493-3544-2.

Publisher's Note: MDPI stays neutral with regard to jurisdictional claims in published maps and institutional affiliations.



© 2020 by the authors. Licensee MDPI, Basel, Switzerland. This article is an open access article distributed under the terms and conditions of the Creative Commons Attribution (CC BY) license (<http://creativecommons.org/licenses/by/4.0/>).